



Exploiting Discontinuities in Optical Flow

WILLIAM B. THOMPSON

Department of Computer Science, University of Utah, Salt Lake City, UT 84112

thompson@cs.utah.edu

Received November 29, 1995; Accepted June 2, 1998

Abstract. Most optical flow estimation techniques have substantial difficulties dealing with flow discontinuities. Methods which simultaneously detect flow boundaries and use the detected boundaries to aid in flow estimation can produce significantly improved results. Current approaches to implementing these methods still have important limitations, however. We demonstrate three such problems: errors due to the mixture of image properties across boundaries, an intrinsic ambiguity in boundary location when only short sequences are considered, and difficulties insuring that the motion of a boundary aids in flow estimation for the surface to which it is attached without corrupting the flow estimates for the occluded surface on the other side. The first problem can be fixed by basing flow estimation only on image changes at edges. The second requires an analysis of longer time intervals. The third can be aided by using a boundary detection mechanism which classifies the sides of boundaries as occluding and occluded at the same time as the boundaries are detected.

Keywords: visual motion, optical flow, discontinuities, edges

1. Introduction

Discontinuities in optical flow are normally viewed as a serious impediment to producing accurate estimates of the flow. Due to the ambiguous nature of flow within small space-time neighborhoods of an image sequence, all methods for estimating flow either explicitly or implicitly assume some sort of spatial and/or temporal continuity. This assumption is often violated at surface boundaries. This paper points out important shortcomings in one class of methods for estimating possibly discontinuous optical flow and indicates how improvements can be made.

Two general approaches to dealing with flow discontinuities are found in the literature. The first explicitly allows for a mixed distribution near boundaries. Marr and Poggio (1977) and Barnard and Thompson (1980) did this by basing their analyses on prominent modes of possible disparities over local neighborhoods. Us-

ing currently popular terminology, the modes acted as a *robust estimator* for the dominant disparity in the neighborhood, though neither paper explained this effect. Some years later, Prazdny (1985) made the idea explicit. Scott's principal component approach (Scott, 1988) and Schunck's constraint line clustering (Schunck, 1989) utilized the same concept. More recently, Black and Anadan (1990) explicitly used robust estimation in determining optical flow near boundaries. Bergen *et al.* (1990) used a more specialized approach in which one dominant motion is found first and then used to produce a new image sequence in which the found motion is nulled, allowing a second motion to be more easily estimated. Once flow is estimated using any of the above approaches, it is relatively straightforward to find the flow discontinuities (Thompson, 1985).

The second approach is to make discontinuities explicit, thus avoiding the need to deal with mixed distri-

butions. All of these methods follow the basic structure of Geman and Geman (1984) or Blake and Zisserman (1987). The most common approach utilizes a Markov random field (MRF) formulation with explicit line processes (Murray and Buxton, 1987; Gamble and Poggio 1987; Hutchinson *et al.*, 1988; Koch *et al.*, 1989; Konrad and Dubois, 1992; Heitz and Bouthemy, 1993). Interacting region and line processes are involved. The region processes combine information over local neighborhoods to reduce ambiguity and improve reliability of individual flow estimates. The line processes estimate locations of discontinuities and act to keep points on opposite sides from interacting in the region processes. The estimation of discontinuities can be greatly assisted if independent information about possible surface boundaries is available. In particular, most of the papers referenced above allow the assertion of a boundary element only at locations likely to correspond to contrast edges.

This paper addresses optical flow estimation using explicit discontinuity detection. We provide evidence for three claims:

- Line processes, as usually implemented, do not completely remove undesirable interactions between surfaces on either side of a motion boundary.
- There is an intrinsic ambiguity in the localization of motion boundaries which can only be resolved over multiple frame pairs.
- Distinguishing between the *occluding* and *occluded* sides of an optical flow boundary can aid the flow estimation process.

Ways of exploiting these observations are demonstrated using a simple flow estimation procedure. They can easily be incorporated into more complete flow estimation systems.

2. Estimating Optical Flow in the Presence of Discontinuities

Existing flow estimation techniques which involve explicit motion boundary detection suffer from two deficiencies when applied to image sequences with textured backgrounds. Interactions between surfaces on either side of the boundary can still occur, degrading the accuracy of the estimated flow. Furthermore, motion boundary detection itself is subject to a localization ambiguity when only a single frame pair is analyzed at a time.

2.1. Mixed image properties near the boundary

Clearly, optical flow cannot be determined based only on a single space/time image point. All methods for estimating optical flow use image properties that must be computed over neighborhoods. Gradient-based techniques (e.g., Fennema and Thompson, 1979; Horn and Schunck, 1981) require the estimation of spatial and temporal derivatives using some form of finite difference. Region-based methods (e.g., Anandan, 1989) compare local neighborhoods around selected points in each frame. Space-time filtering methods (e.g., Adelson and Bergen, 1986; Heeger, 1988; Fleet and Jepson, 1990) are implemented using FIR filters with finite spatial and temporal extent. Image properties are often computed after some form of pre-filtering (Kearney *et al.*, 1987; Barron *et al.*, 1994) also involving operations with finite spatial and/or temporal extent. In addition, many flow estimation methods impose explicit flow continuity constraints (e.g., Fennema and Thompson (1979), Barnard and Thompson (1980), Horn and Schunck (1981), and the various MRF algorithms).

The line processes used to deal with flow discontinuities in MRF-like methods in fact only affect the imposition of explicit flow continuity constraints. Image properties associated with points to one side of an asserted boundary can still be effected by the intensity patterns on the other side of the boundary. Derivatives estimated using finite differences and pre-filtering will have substantial errors in the vicinity of motion boundaries, particularly if the surfaces to one of both sides are highly textured. A similar effect occurs with spatiotemporal filters. While the line processes stop direct interactions between estimated flow to either side of a surface boundary, the flow estimates themselves can still be highly inaccurate.

If done in a systematic manner, the use of adaptive window sizes can reduce the effects of mixed image properties at boundaries (Kanade and Okutomi, 1994; Nagel, 1995). An alternate and more easily implemented solution is to base flow estimates on correctly chosen sparse image features. The features must be lines or points that necessarily occur either well away from surface boundaries or occur exactly at the boundary and for which localization is not significantly effected by image structure to either side of the boundary. The Moravec "interest operator" (Barnard and Thompson, 1980), extrema in the difference of Gaussians (Mutch and Thompson, 1983), corner detectors

(Ranagrajan *et al.*, 1988), and methods based on contrast edges (Hildreth, 1983; Waxman *et al.*, 1988) satisfy this property.

2.2. Ambiguity of surface boundary location

Many of the methods for detecting flow discontinuities are based on looking for large magnitude values of the flow gradient. Unless the location of the flow discontinuity is already known or methods which allow for multiple motions near boundaries are used, estimated flow will be smoothed over near the boundary. Figure 1 illustrates the problem. Estimated flow magnitude is plotted against position along an axis perpendicular to a surface boundary. Away from the boundary, flow estimates will be reasonably accurate. They should also be accurate on the occluding surface near the boundary, since the boundary itself will have sufficient structure to allow flow estimation and is moving with the occluding surface. On the occluded side, however, flow estimates won't be accurate until observed sufficiently far from the boundary to allow the moving texture of the occluded surface to dominate any effects associated with the surface boundary, which is moving with a different optical flow. The maximum rate of change in flow will typically be noticeably offset from the actual boundary.

Whatever flow-based boundary detection method is used, there is an intrinsic localization ambiguity associated with instantaneous flow that cannot be overcome without either non-motion cues to the boundary location or analysis over longer time intervals (Thompson and Barnard, 1981).¹ Consider the pattern shown on the left in Figure 2. Three bars, α , β , and γ , are moving to the left. Three other bars, **a**, **b**, and **c**, are moving to the right. Assuming that occlusion boundaries are likely to have associated contrast edges, then the edge of the occluding surface is either along the right side of bar γ or the left side of bar **c**. Without additional information, there is no way to resolve this ambiguity. Not until the next time step, shown on the right in the figure, is it apparent that the lighter colored bars on the left are occluding the darker colored bars to the right and that the true occlusion boundary is at the edge of bar γ . This problem affects not only boundary detection based on flow gradients, but also methods which are based on the appearance and disappearance of surface texture (Kaplan, 1969; Mutch and Thompson, 1985), methods which allow for multi-

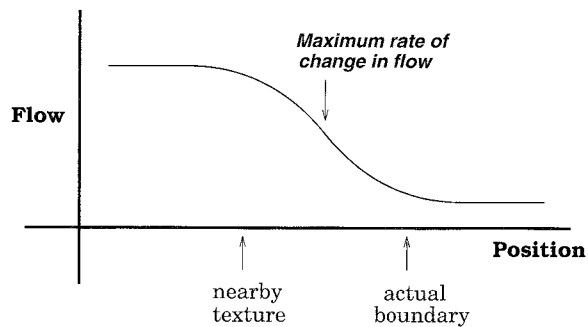


Fig. 1. Optical flow gradients are not sufficient to accurately locate flow boundaries.

ple motions within a local neighborhood, and methods which attempt to recognize occlusion boundaries using properties of similarity surfaces (e.g., Anandan, 1989). A method for deciding which possibility – bar γ , bar **c**, or the newly appeared bar **d** – really corresponds to the surface boundary is described in section 3.2.1.

3. An Algorithm for Flow Estimation in the Presence of Discontinuities

This section outlines an optical flow estimation algorithm which effectively addresses the problems discussed in section 2. It has similarities to the method presented in Heitz and Bouthemy (1993), though differs in a number of important regards: the algorithm correctly deals with mixed image properties near surface boundaries, it uses a more complete classification of boundary types, and it is able to resolve boundary ambiguities when textured backgrounds are present. The algorithm utilizes explicit line processes to avoid undesirable interactions across motion discontinuities in a manner analogous to the MRF methods, but using a much simpler formulation. The important features of this algorithm can be added to most existing flow estimation approaches.

In the remainder of this paper, our analysis excludes motions consisting exclusively of rotations of revolute objects around an axis perpendicular to the line of sight and corresponding to the axis of symmetry of the object. This particular situation introduces additional ambiguities, the resolution of which is still largely an open question (Thompson *et al.*, 1992; Thompson and Painter, 1992).

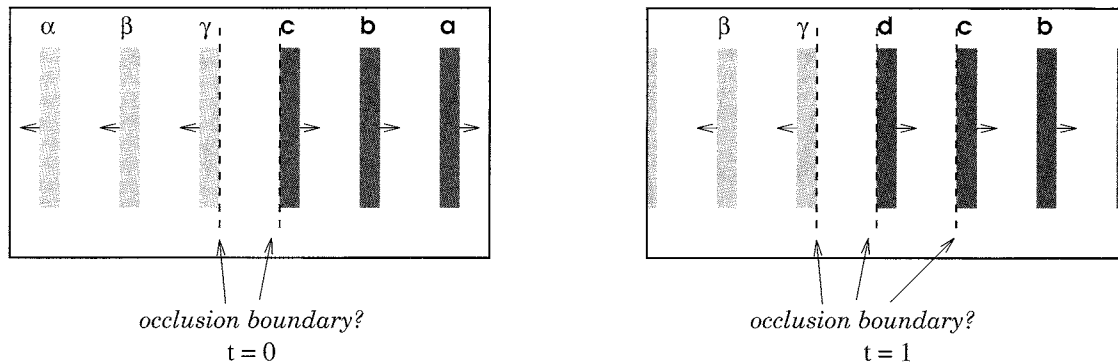


Fig. 2. Intrinsic ambiguity in boundary location at one instant in time.

3.1. Dealing with discontinuities

At flow discontinuities, effective flow estimation methods must avoid smoothing the flow across the boundary and must also keep image properties associated with a surface on one side of the boundary from corrupting the flow estimation for the surface on the other side. We deal with this second problem by basing flow estimation solely on image features which are relatively unaffected by this mixture of image properties. In particular, we base flow calculations only on image properties at edges. As long as no temporal pre-filtering is performed, spatial contrast edges will either be close approximations to surface boundaries or far enough away from surface boundaries so that local image properties near the edge are largely unaffected by image regions that are part of other surfaces. This has the additional advantage of minimizing difficulties due to apparent misregistrations between contrast and motion edges due to localization errors when separate image primitives are used. The standard Horn and Schunck (1981) method is utilized, modified so that spatial and temporal image gradients are only used at spatial edges. For other image locations, flow is estimated using the interpolation properties intrinsic to the method.

Given information about the location of surface boundaries, it is straightforward to avoid flow computation interactions across boundaries. The Gauss-Seidel method used in the basic Horn and Schunck algorithm bases flow estimates for a given pixel at a particular iteration step on the average values at neighboring pixels in the previous iteration. It is only necessary to make sure this average does not include any pixels on the other side of a motion discontinuity.

Discontinuity detection is based on an analysis of flow differences across contrast edges which poten-

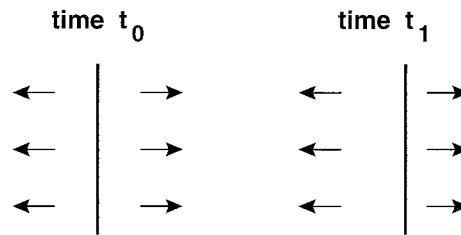


Fig. 3. The surface to the left has an optical flow different from that of the boundary and hence is an occluded surface. Since it is moving away from the boundary, it is in fact being disoccluded.

tially signal surface boundaries. When possible, the surfaces to either side of a detected boundary are classified as *occluding* or *occluded* using the *boundary flow constraint*, which states that the flow associated with the occluding surface immediately adjacent to the boundary will be equal to the flow of the boundary (Thompson *et al.*, 1985). Violations of the boundary flow constraint can be used to identify occluded or disoccluded surfaces, as shown in Figure 3, without any need to know the camera or object motions involved. This relationship is only useful when there are differences across the boundary in the component of flow normal to the boundary. If the flows to either side of a boundary are parallel to the boundary itself, then it is not possible to determine which side is occluding the other without additional information about camera motion. Such *sheer boundaries* still indicate occlusion, however.

To detect and classify motion boundaries, the flow associated with every point on a contrast edge is compared to the flow to either side. The flows to either side are separated into components normal to the edge orientation, f_1^\perp and f_2^\perp and parallel to the edge, f_1^\parallel and f_2^\parallel . Detection and classification proceeds by first checking to see if one surface is progressively occlud-

ing or disoccluding the other. If not, sheering surfaces are checked for:

```

 $d_1^\perp = |f_1^\perp - f^\perp|$ ,  $d_2^\perp = |f_2^\perp - f^\perp|$ 
if  $\max(d_1^\perp, d_2^\perp) \geq T_1$ 
  if  $d_1^\perp > d_2^\perp$ 
    side 1 is occluded, side 2 is
    occluding
  else
    side 1 is occluding, side 2 is
    occluded.
else if  $|f_1^\parallel - f_2^\parallel| \geq T_2$ 
  sides 1 and 2 are sheer

```

This method, while less elegant than the detection and classification scheme described in Thompson *et al.* (1985) is more reliable. Note in particular that f_1^\perp and f_2^\perp are separately compared to the normal flow of the edge, rather than just taking their difference. This is important, as it increases the sensitivity of the edge detection. Because of the effects described in section 2.2, the difference in flow normal to the edge attributable to one surface moving relative to another will be concentrated in d_1^\perp or d_2^\perp . Additional differences in flow normal to the edge will arise due to smooth variations in flow on the occluding side of the edge and from various noise effects. As a result, basing detection on $|f_1^\perp - f_2^\perp|$ will increase the classification error rate.

Flow estimation at a boundary pixel neither affects nor is affected by the flow at pixels to the occluding side of the boundary. Interactions to the occluding side, however, are allowed, since the boundary is part of that surface. A conservative approach is taken for sheer boundaries. The flow estimation at the boundary is isolated from the flow values to either side, but does interact with the estimation of other values along the boundary. The complete algorithm interleaves flow

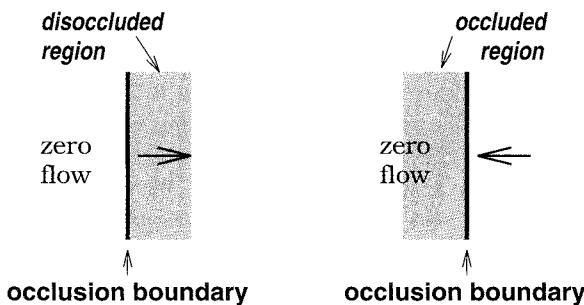


Fig. 4. Projecting flow into occlusion and disocclusion regions.

estimation and boundary detection. Enough Gauss-Seidel iterations are done to get a reasonable estimate of flow values. Boundaries are then detected and classified. Better flow estimates are obtained by performing additional iterations using this information. The process is repeated as necessary.

3.2. Improving boundary localization over time

Optical flow estimation over sequences longer than a single frame pair can improve the efficiency of iterative algorithms by providing reasonably accurate initial values and can improve the accuracy of many methods by using some form of temporal coherence to reduce the effects of noise. It turns out that longer sequences are also the key to resolving the localization ambiguity described in section 2.2.

3.2.1. Boundary projection Surface boundaries persist over time. Once these boundaries are found at one time step, their position can be easily predicted for the next time step. This is done by taking each point on a detected occlusion boundary and looking for a contrast edge in the future frame at the corresponding location, offset by the flow of the boundary point. Substantial efficiency is achieved by starting the iterations at the next time step using these predicted boundary locations. Even more importantly, over time actual surface boundaries will be maintained while detected boundaries that in fact correspond to surface texture near true boundaries will disappear.

To see why this is so, consider Figure 2. At time step 0, the interleaved iterate and classify algorithm will end up finding potential occlusion boundaries to the right of bar γ and to the left of bar \mathbf{c} . The flow estimates assigned to the region between the bars is likely to be a muddle. At time step 1, bar \mathbf{d} has appeared. The flow of this new “texture element” will initially propagate both left and right, since there is no surface boundary indication associated with the bar. As the flow propagation approaches bar \mathbf{c} , the differential flow across the (false) boundary on the left side of \mathbf{c} is reduced, leading to a reclassification of the edge as non-occluding. The sides of \mathbf{d} never get classified as occluding, since the only flow not consistent with the edge motion is blocked by the boundary at γ from propagating towards \mathbf{d} . The situation shown in Figure 2 is extreme in that a full texture element appears over a single time step. In practice, texture element spacing



Fig. 5. Original image sequence, frames 1 – 4.

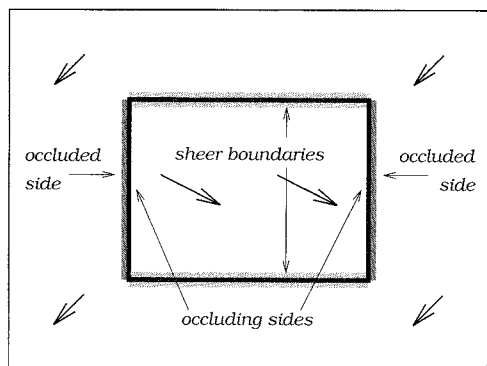


Fig. 6. “True” boundary classifications for moving rectangle test sequence.

is usually much larger than inter-frame motions and the effect described above takes place more gradually.

3.2.2. Flow projection Horn and Schunck suggest improving the efficiency of their algorithm by using the results obtained for one time step to initialize the iterations at the next time step. Simply using the flow obtained for each pixel at one time step to initialize the estimates for the same pixel at the next time step is adequate over smooth surfaces, but can actually lead to worse results at occlusion boundaries than if a default of zero flow is used in the initialization. This is because the flow associated with a disoccluded surface region will typically be very different from the flow of the surface which was previously occluding it. Some improvement can be obtained by projecting the flow estimates at one time step to pixels in the next time in a manner that takes into account the flow value itself. This fails, however, to provide initial estimates for flow in occluded regions where multiple flow values project to the same point and in disocclusion regions where no flow values from the previous time step will project (Black and Anandan, 1990).

Effective projection of flow into occluded and disoccluded regions in the next time step is possible if occlusion boundaries have been detected and classified in the current time step. Figure 4 shows a simplified situ-

ation in which an occlusion boundary is stationary, the occluding surface is to the left, the occluded surface is to the right, and the motion of the occluded surface is normal to the boundary. Two possibilities exist: the occluded surface is moving either towards or away from the boundary. (In the case of pure shear motion, no occlusion or disocclusion regions exist.) Movement away from the boundary causes disocclusion. The gray area on the left of Figure 4 indicates the region in the next time step that will correspond to surface visible for the first time and which will have flow close to that on the occluded side of the boundary. Movement towards the boundary causes occlusion. The gray area on the right in Figure 4 indicates the region in the next time step where flow vectors from two different surfaces will both project. The best estimate of the actual flow will be the flow of the boundary itself. In either case, the region of occlusion/disocclusion runs from the boundary to a line found by adding the flow vector of the occluded surface point nearest each boundary point to the boundary point location. For the more general case of moving boundaries, the region of occlusion/disocclusion runs from the projection of the boundary into the next time step to the line found by adding the flow vector of the occluded surface point nearest each boundary point to the projected boundary point location. The flow to be filled into these regions is either the flow of the boundary or the flow of the nearest occluded surface point, depending on the classification of the boundary.

Note that the principal goal here is to improve efficiency, not implement some sort of temporal continuity constraint. Temporal consistency can also be used to improve accuracy in flow estimation, though this constraint can lead to problems in occlusion/disocclusion regions (Murray and Buxton, 1987). Thus, the approach described in the preceding paragraph might be extended to better exploit temporal continuity at and near boundaries.

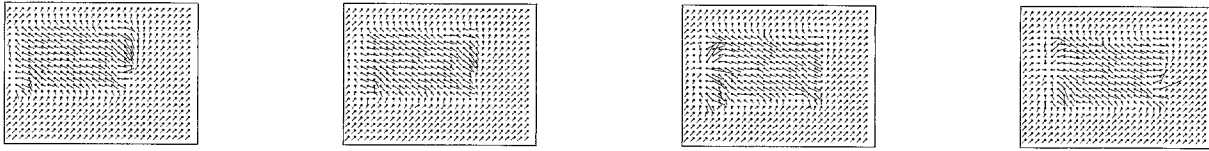


Fig. 7. Flow estimation using standard Horn and Schunck method (first four frame pairs).

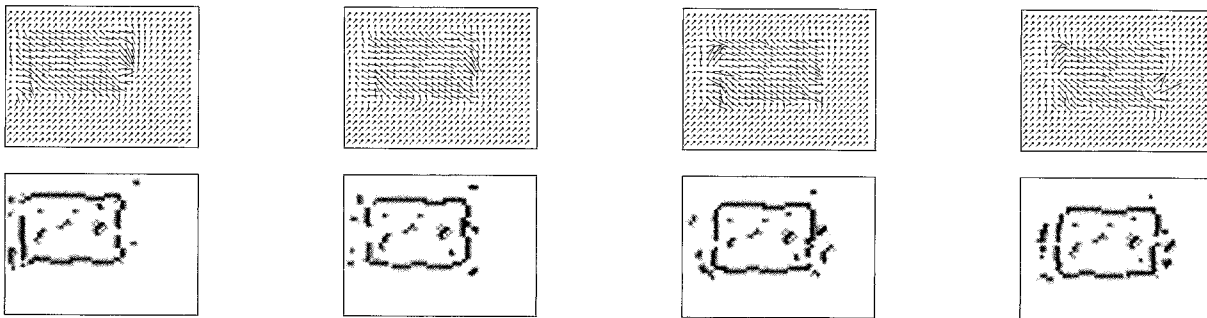


Fig. 8. Flow estimation using Horn and Schunck with explicit boundary detection (first four frame pairs).

4. Experimental Results

This section presents results from controlled experiments run on synthetic data. Implementation details and results on real imagery are presented in Thompson (1995). While the limitations of using synthetic data are well known, it is the only way to do fair quantitative comparisons between alternate approaches. The accuracy of estimated flow was measured using the inter-frame angular deviation described in Barron, 1994. While this measure is useful in evaluating the results of the controlled experiments described below, the absolute magnitudes of flow errors should not be compared with those obtained in other circumstances. In the tests reported here, most of the flow estimation error occurs at flow discontinuities, which correspond to a substantial number of the pixels in the test sequences. This is not the case with other image sequences, such as those used in Barron, 1994. Error magnitude comparisons between dissimilar image sequences will be dominated by the number of pixels at or near discontinuities at least as much as by the quality of the flow estimation algorithms applied.

In evaluating the results, it is also important to note that the performance of the methods described here de-

pends on both the particular motion analysis algorithm used and the quality of the (static) edges on which it is based. In order to provide a grounds for comparing algorithms, a simple edge detector was used and manipulations of the test sequences were structured to avoid perturbations of edge detector performance. For example, sub-pixel motions were avoided, since edge detector results would be affected by the anti-aliasing scheme used to generate synthetic images with non-integral motions. To get the best possible performance, as would be desirable if quantitative comparisons were been done with competing methods, a more sophisticated edge detector should be used.

Figure 5 shows the first four images from an 120 by 160 pixel synthetically generated sequence with a textured rectangle moving across a textured background. The rectangle is moving four pixels to the right and two pixel down per frame. The background is moving two pixel down and to the left per frame. Figure 6 shows the true occluded/occluding and sheer boundaries for this sequence. In this and subsequent figures, sheer boundaries are marked by a light gray pattern on either side of a dark line while occluded/occluding boundaries are marked by a darker gray pattern on the occluded side of the edge.

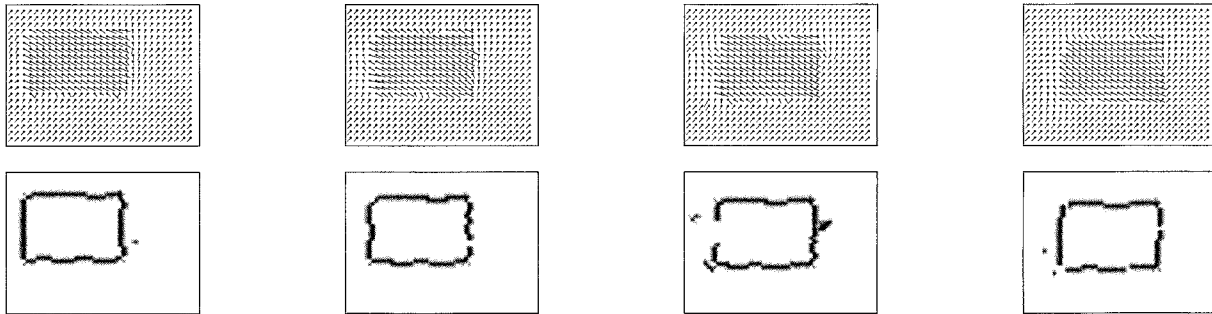


Fig. 9. Edge-based flow estimation using explicit discontinuity detection.

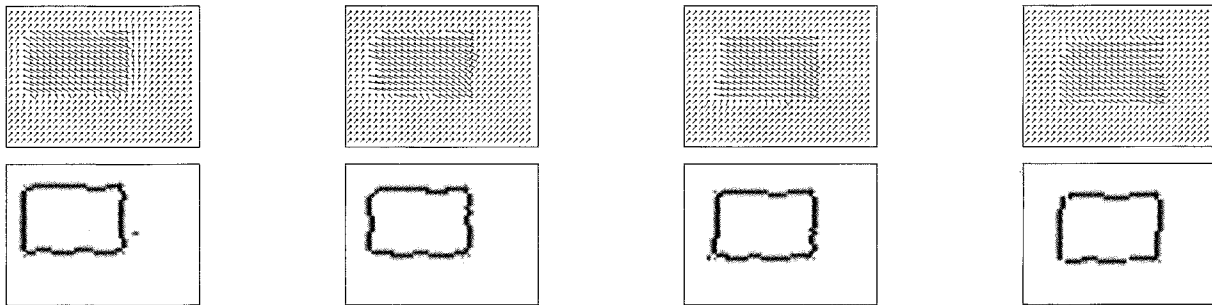


Fig. 10. Flow estimation using explicit discontinuity detection and projection.

Figure 7 shows the optical flow estimated by the standard Horn and Schunck algorithm, applied to the first four frame pairs of the moving rectangle sequence. The errors in flow estimation, particularly at and near the boundaries of the moving rectangle, are obvious. Figure 8 demonstrates the results of adding explicit boundary analysis to the basic Horn and Schunck algorithm. The final flow estimates and boundary classifications at each time step are shown. While the flow estimates are improved, substantial error remains due to the mixing of image properties across the boundaries, which seriously distorts the gradient computations. Figure 9 uses the same algorithm as Figure 8, except that only image properties at contrast edges are used in the flow computations. This minimizes the effects of image property mixing between surfaces. Results for four frame pairs are shown. Flow estimates are further improved. The ambiguity in detecting and classifying boundaries when background texture appears near occluding contours, which is manifested in the figure as missing and extraneous boundary segments, is still af-

fecting accuracy, however. Figure 10 shows the effect of using boundary projection to initialize processing at the next time step. The boundary classification errors have largely been eliminated and the flow estimates correspondingly improved. Table 1 lists the quantitative average errors associated with each of these algorithms.

The next set of experiments tests the value of classifying surface boundaries by labeling the sides as occluding or occluded. A test sequence consisting of a uniform intensity disk moving over a textured background was used, with foreground and background motions as in the previous tests (Figure 11). To insure convergence given the large, uniform brightness area, 600 iterations were run at every time step. Occluding/occluded boundary classification should allow the motion of the disk boundary itself to propagate into the otherwise featureless interior of the disk. As is clear in Table 2, accuracy is improved.

Table 1. Flow errors for different estimation algorithms.

frame pair:	1	2	3	4	5	6	7	8
Basic Horn and Schunck	13.38°	14.05°	15.91°	15.62°	13.14°	15.52°	13.84°	13.43°
Horn and Schunck with boundary detection	11.31°	11.75°	13.27°	12.88°	11.18°	13.90°	11.77°	10.88°
Edge-based flow estimation with boundary detection	7.55°	8.28°	8.76°	7.15°	10.38°	9.74°	9.02°	7.09°
Edge-based flow est. with boundary detection, projection	7.55°	5.35°	4.75°	4.65°	5.28°	5.29°	4.81°	4.25°

Table 2. Flow errors using symmetric and asymmetric boundary classification.

frame pair:	1	2	3	4	5	6	7	8
Symmetric boundary classification	6.75°	9.32°	8.51°	5.28°	5.40°	6.62°	6.81°	7.07°
Asymmetric boundary classification	5.55°	7.26°	7.00°	3.86°	4.07°	4.67°	4.95°	5.50°

The final set of experiments address the issue of how well projecting the estimated flow from one time step to initialize computations at the next time step helps in flow determination. The image sequence used was that shown in Figure 5. A total of 30 iterations were run at each time step, as compared to 150/step for the results shown in Figures 7-10. Five cases were examined, with the resulting errors shown in Table 3. For the first case, the algorithm employing boundary classification and boundary projection was used as in Figure 10, only with the reduced number of iterations. In the second case, no boundary projection was done, but flow in each time step after the first was initialized copying the values obtained in the previous time step. (While boundaries were not projected from frame to frame, boundary detection and classification was used within each time step.) With reduced iteration, initializing flow estimates is clearly more valuable than initializing boundary estimates. In the third test, there was no boundary projection and flow estimates were initialized using the projection method described in section 3.2.2. There is a substantial improvement in accuracy. The last two cases use boundary projection and flow that is

initialized by either copying or projecting values from the previous time step. Again, flow projection is clearly superior to simple copying.

5. Summary

This paper has examined a number of important issues affecting the accuracy of optical flow estimates made by algorithms which explicitly take into account flow discontinuities. Theoretical and experimental evidence has been presented showing that the line processes typically used to keep flow smoothness constraints from corrupting estimates across boundaries can still allow image properties associated with a surface to one side of a boundary to improperly influence flow computations on the other side of the boundary. A second problem affecting flow estimation is the intrinsic ambiguity of boundary localization in textured environments when only two frames are considered at a time. This effect was clearly demonstrated using one particular flow estimation algorithm, but occurs independent of the algorithm used. Experimentation has shown the value of distinguishing between occluding and occluded sides of a surface corresponding to a flow discontinuity. This

Table 3. Flow errors when total iterations are reduced.

frame pair:	1	2	3	4	5	6	7	8
Boundary projection, no flow projection	21.99°	22.95°	22.37°	23.28°	22.74°	23.24°	22.65°	21.15°
No boundary projection, copied flow	21.99°	14.93°	13.46°	12.53°	12.43°	12.66°	12.25°	12.26°
No boundary projection, projected flow	21.99°	15.88°	13.34°	11.89°	11.29°	11.06°	10.96°	9.96°
Boundary projection, copied flow.	21.99°	14.47°	11.59°	10.23°	10.07°	9.50°	9.06°	9.39°
Boundary projection, projected flow.	21.99°	15.01°	10.86°	8.74°	7.58°	7.04°	6.67°	5.56°

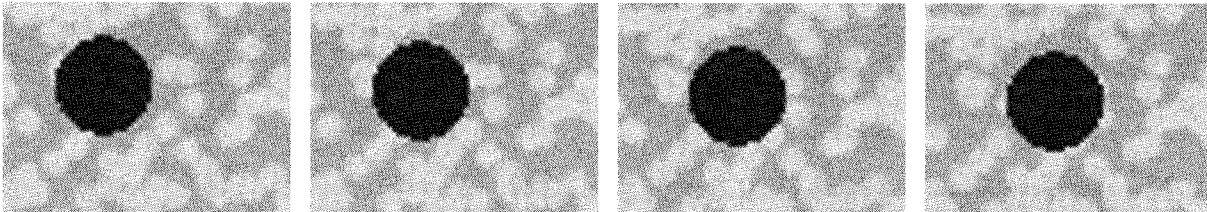


Fig. 11. Moving disk image sequence.

information can be used to improve flow estimates and is important in projecting flow estimates to future time steps so as to reduce computational requirements. Finally, we have shown how the line processes used in MRF formulations for estimating optical flow can also be used in the conceptually simpler Horn and Schunck algorithm. While the techniques we have described for improving flow estimation at boundaries are most easily implemented in algorithms such as Horn and Schunck and MRF methods, they can be applied across the spectrum of approaches to optical flow estimation. For example, the area correlation algorithm described in Smitley and Bajcsy (1981) can be viewed as utilizing something akin to a line process when matching image regions.

Acknowledgements

This work was supported by National Science Foundation grant IRI-9112267.

Notes

1. There is evidence that the human vision system resolves this ambiguity by favoring whichever possible boundary has the strongest non-motion edge properties (Yonas, 1990).

References

- Adelson, E.H. and Bergen, J.R. 1986. The extraction of spatio-temporal energy in human and machine vision. In *Proc. Workshop on Motion: Representation and Analysis*, pages 151–155.
- Anandan, P. 1989. A computational framework and an algorithm for the measurement of visual motion. *International Journal of Computer Vision*, pages 283–310.
- Barnard, S.T. and Thompson, W.B. 1980. Disparity analysis of images. *IEEE Trans. on Pattern Analysis and Machine Intelligence*, PAMI-2:333–340.
- Barron, J.L., Fleet, D.J. and Beauchemin, S.S. 1994. Performance of optical flow techniques. *International Journal of Computer Vision*, pages 43–77.
- Bergen, J.R., Burt, P.J., Hingorani, R. and Peleg, S. 1990. Computing two motions from three frames. In *Proc. Third International Conference on Computer Vision*, pages 27–32.
- Black, M.J. and Anandan, P. 1990. A model for the detection of motion over time. In *Proc. Third International Conference on Computer Vision*, pages 33–37.

- Blake, A. and Zisserman, A. 1987. *Visual Reconstruction*. MIT Press, Cambridge, MA.
- Fennema, C.L. and Thompson, W.B. 1979. Velocity determination in scenes containing several moving objects. *Computer Graphics and Image Processing*, 9:301–315.
- Fleet, D.J. and Jepson, A.D. 1990. Computation of component image velocity from local phase information. *International Journal of Computer Vision*, pages 77–104.
- Gamble, E. and Poggio, T. 1987. Visual integration and detection of discontinuities: The key role of intensity edges. AI Memo 970, MIT.
- Geman, S. and Geman, D. 1984. Stochastic relaxation, Gibbs distributions, and the Bayesian restoration of images. *IEEE Trans. on Pattern Analysis and Machine Intelligence*, PAMI-6:721–741.
- Heeger, D.J. 1988. Optical flow estimation using spatiotemporal filters. *International Journal of Computer Vision*, pages 279–302.
- Heitz, F. and Bouthemy, P. 1993. Multimodal estimation of discontinuous optical flow using markov random fields. *IEEE Trans. on Pattern Analysis and Machine Intelligence*, 15:1217–1232.
- Hildreth, E.C. 1983. *The Measurement of Visual Motion*. MIT Press, Cambridge, MA.
- Horn, B.K.P. and Schunck, B. 1981. Determining optical flow. *Artificial Intelligence*, 17:185–203.
- Hutchinson, J., Koch, C., Luo, J. and Mead, C. 1988. Computing motion using analog and binary resistive networks. *Computer*, 21:52–63.
- Kanade, T. and Okutomi, M. 1994. A stereo matching algorithm with an adaptive window: Theory and experiment. *IEEE Trans. on Pattern Analysis and Machine Intelligence*, 16(9):920–932.
- Kaplan, G.A. 1969. Kinetic disruption of optical texture: The perception of depth at an edge. *Perception & Psychophysics*, 6(4):193–198.
- Kearney, J.K., Thompson, W.B. and Boley, D.L. 1987. Optical flow estimation: An error analysis of gradient-based methods with local optimization. *IEEE Trans. on Pattern Analysis and Machine Intelligence*, PAMI-9:229–244.
- Koch, C., Wang, H.T., Mathur, B., Hsu, A., and Suarez, H. 1989. Computing optical flow in resistive networks and in the primate visual system. In *Proc. Workshop on Visual Motion*, pages 62–69.
- Konrad, J. and Dubois, E. 1992. Bayesian estimation of motion vector fields. *IEEE Trans. on Pattern Analysis and Machine Intelligence*, 14:910–927.
- Marr, D. and Poggio, T. 1979. Cooperative computation of stereo disparity. *Science*, 194:283–287.
- Murray, D.W. and Buxton, B.F. 1987. Scene segmentation from visual motion using global optimization. *IEEE Trans. on Pattern Analysis and Machine Intelligence*, PAMI-9:220–228.
- Mutch, K.M. and Thompson, W.B. 1983. Hierarchical estimation of spatial properties from motion. In A. Rosenfeld, editor, *Multiresolution Image Processing and Analysis*, pages 343–354. Springer-Verlag.
- Mutch, K.M. and Thompson, W.B. 1985. Analysis of accretion and deletion at boundaries in dynamic scenes. *IEEE Trans. on Pattern Analysis and Machine Intelligence*, PAMI-7:133–138.
- Nagel, H.H. 1995. Optical flow estimation and the interaction between measurement errors at adjacent pixel positions. *International Journal of Computer Vision*, 15(3):273–288.
- Prazdnyk, K. 1985. Detection of binocular disparities. *Biological Cybernetics*, 52:93–99.
- Rangarajan, K., Shah, M. and Van Brackle, D. 1988. Optimal corner detection. In *Proc. Second International Conference on Computer Vision*, pages 90–94.
- Schunck, B.G. 1989. Image flow segmentation and estimation by constraint line clustering. *IEEE Trans. on Pattern Analysis and Machine Intelligence*, PAMI-11:1010–1027.
- Scott, G.L. 1988. *Local and Global Interpretation of Moving Images*. Morgan Kaufman, Los Altos.
- Smitley, D.L. and Bajcsy, R. 1984. Stereo processing of aerial, urban images. In *Proc. Seventh Int. Conference on Pattern Recognition*, pages 433–435.
- Thompson, W.B. 1995. Exploiting discontinuities in optical flow. Technical Report UUCS-95-015, Department of Computer Science, University of Utah.
- Thompson, W.B. and Barnard, S.T. 1981. Lower-level estimation and interpretation of visual motion. *Computer*, 14:20–28.
- Thompson, W.B., Kersten, D. and Knecht, W.R. 1985. Structure-from-motion based on information at surface boundaries. *Biological Cybernetics*, pages 327–333, 1992.
- Thompson, W.B., Mutch, K.M. and Berzins, V.A. 1985. Dynamic occlusion analysis in optical flow fields. *IEEE Trans. on Pattern Analysis and Machine Intelligence*, PAMI-7:374–383.
- Thompson, W.B. and Painter, J.S. 1992. Qualitative constraints for structure-from-motion. *Computer Vision, Graphics and Image Processing: Image Understanding*, pages 69–77.
- Waxman, A.M., Wu, J. and Bergholm, F. 1988. Convected activation profiles and the measurement of visual motion. In *Proc. IEEE Conference on Computer Vision and Pattern Recognition*, pages 717–723, Ann Arbor, MI.
- Yonas, A., Craton, L.G., Thompson, W.B. and Condry, K.F. 1990. Boundary identification and the computation of relative motion: Two processes in kinetic occlusion. *Abstracts in Investigative Ophthalmology and Visual Science*, 31(4):524.

